Gene Therapy (2014) **21**, 566–574
© 2014 Macmillan Publishers Limited All rights reserved 0969-7128/14
www.nature.com/gt

ORIGINAL ARTICLE

Exploitation of Langerhans cells for *in vivo* DNA vaccine delivery into the lymph nodes

ER Tőke[1,8], O Lőrincz[1,8], Z Csiszovszki[1,8], E Somogyi[1,8], G Felföldi[1,9], L Molnár[1,8], R Szipőcs[2,3], A Kolonics[2,3], B Malissen[4], F Lori[5,8,10], J Trocio[5,11], N Bakare[5,12], F Horkay[6], N Romani[7], CH Tripp[7], P Stoitzner[7] and J Lisziewicz[1,8]

There is no clinically available cancer immunotherapy that exploits Langerhans cells (LCs), the epidermal precursors of dendritic cells (DCs) that are the natural agent of antigen delivery. We developed a DNA formulation with a polymer and obtained synthetic 'pathogen-like' nanoparticles that preferentially targeted LCs in epidermal cultures. These nanoparticles applied topically under a patch-elicited robust immune responses in human subjects. To demonstrate the mechanism of action of this novel vaccination strategy in live animals, we assembled a high-resolution two-photon laser scanning-microscope. Nanoparticles applied on the native skin poorly penetrated and poorly induced LC motility. The combination of nanoparticle administration and skin treatment was essential both for efficient loading the vaccine into the epidermis and for potent activation of the LCs to migrate into the lymph nodes. LCs in the epidermis picked up nanoparticles and accumulated them in the nuclear region demonstrating an effective nuclear DNA delivery *in vivo*. Tissue distribution studies revealed that the majority of the DNA was targeted to the lymph nodes. Preclinical toxicity of the LC-targeting DNA vaccine was limited to mild and transient local erythema caused by the skin treatment. This novel, clinically proven LC-targeting DNA vaccine platform technology broadens the options on DC-targeting vaccines to generate therapeutic immunity against cancer.

Gene Therapy (2014) **21,** 566–574; doi:10.1038/gt.2014.29; published online 3 April 2014

INTRODUCTION

Innovative vaccines to treat cancer are designed to target dendritic cells (DCs), the main inducers and regulators of the immune system.[1] Epidermal Langerhans cells (LCs) are DCs specialized in the delivery of antigens to lymph nodes in order to induce cytotoxic T-lymphocytes (CTLs) capable of specific killing of tumor cells.[2–6] Relatively few vaccines are administered to the epidermis and there is no vaccine that effectively and selectively targets the LCs before they migrate to the lymph nodes.[7] Vaccines that express antigens from a plasmid DNA (pDNA) do not require cross-priming to induce CTL responses. Therefore, preferential delivery of pDNA to LCs may result in more robust CTL responses than priming these cells with peptides or proteins.[7,8] Unfortunately, inefficient uptake and intracellular degradation of pDNA limits the efficacy of both antigen expression and induction of CTL responses.[9]

We present here the mechanism of action of a clinically proven vaccine technology platform that was developed to harness the immunological function of LCs, to transport antigens from the periphery into the lymph nodes and induce robust CTL responses. The underlying premise of this approach is provided by *ex vivo* manipulation of the DCs that generates optimally activated antigen-presenting cells and a superior method for stimulating clinically significant antitumor and antiviral immunity as compared with more traditional vaccination methods. The platform technology has two key components: (1) LC-targeting nanoparticles that optimized for cellular entry and nuclear delivery of the pDNA for potent expression of antigens; (2) the nanoparticle vaccine formulation is combined with a medical device developed for *in vivo* LC-targeting vaccination. The first LC-targeting vaccine (DermaVir) was safe and induced potent and long-lasting memory CTL responses in human subjects as tested in three clinical trials for infectious disease indications.[10–12] Any DNA incorporated into nanoparticles would induce similar antigen-specific CTL responses because the physico-chemical properties of the LC-targeting nanoparticles are independent on the sequence and size of the encapsulated pDNA.[13] Our translational studies bring corroborating evidences that this technology safely and efficiently deliver pDNA-encoded antigens to the nucleus of LCs, increases their activation and their motility, facilitating antigen delivery to the lymph nodes. Finally, we demonstrate practical and inexpensive clinical applications of the LC-targeting vaccine as an *in vivo* alternative to DC-targeted immunotherapy developed against infectious, neoplastic and autoimmune diseases.

[1]Genetic Immunity Kft, H-1045 Budapest, Hungary; [2]Wigner RCP of HAS, H-1121 Budapest, Hungary; [3]R&D Ultrafast Lasers Ltd, H-1539 Budapest, Hungary; [4]Centre d'Immunologie de Marseille-Luminy, INSERM U1104, CNRS UMR7280, Aix Marseille Université, Marseille, France; [5]Research Institute for Genetic and Human Therapy (RIGHT), Bethesda, MD, USA; [6]Section on Tissue Biophysics and Biomimetics, Eunice Kennedy Shriver National Institute of Child Health and Human Development, NIH, Bethesda, MD, USA and [7]Department of Dermatology and Venereology, Innsbruck Medical University, Innsbruck, Austria. Correspondence: Dr J Lisziewicz, eMMUNITY Inc, 4400 East West Hwy, Bethesda, MD 20814, USA. E-mail: julianna.lisziewicz@emmunityinc.com
[8]Current address: eMMUNITY Inc, 4400 East West Hwy, Bethesda, MD 20814, USA.
[9]Current address: Egis Gyógyszergyár Nyrt. H-1106 Budapest, Keresztúri út 30-38., Hungary.
[10]Current address: ViroStatics srl, 07100 Sassari, Italy.
[11]Current address: Department of Outcomes Research, Pfizer Inc, New York, NY, USA.
[12]Current address: Janssen Research and Development LLC, Titusville, NJ, USA.
Received 15 September 2013; revised 19 January 2014; accepted 17 February 2014; published online 3 April 2014

RESULTS

The size distribution of the vaccine

To develop a new DNA vaccine formulation, we have encapsulated the pDNA within a linear polyethylenimine (PEI) that is modified by covalently bound mannobiose molecules (polyethylenimine-mannose, PEIm) and hypothesized that these pDNA/PEIm nanoparticles are suitable for targeted pDNA delivery to LCs.[13] We investigated the size distribution of these nanoparticles by dynamic light scattering and atomic force microscopy. Size distribution of the Alexa-labeled nanoparticles was comparable to the non-labeled ones. They had a bimodal size distribution profile with two discrete size ranges between 50–100 and 160–240 nm (Supplementary Figures 1a and b).

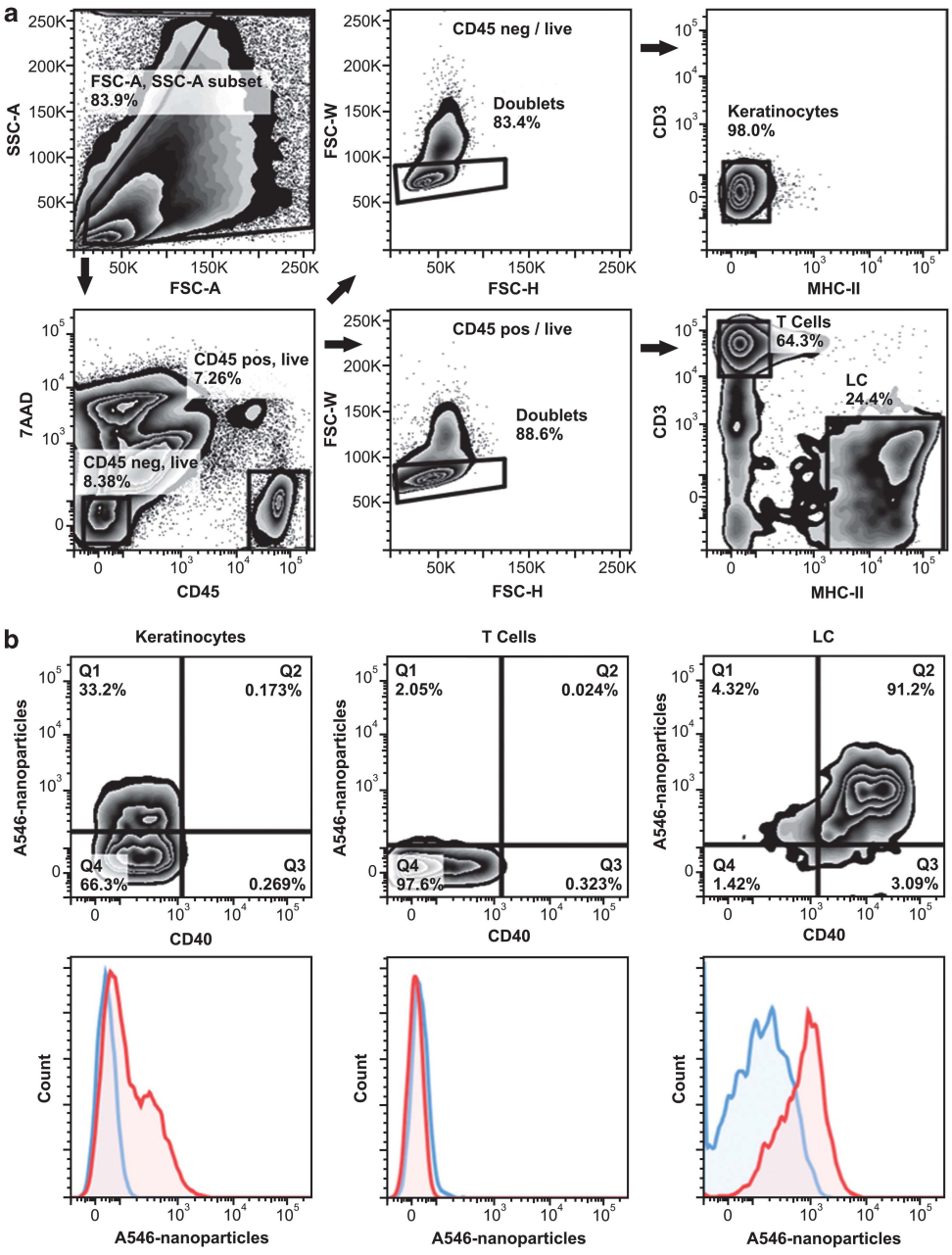

Figure 1. *In vitro* capture of pDNA/PEIm nanoparticles by Langerhans cells (LCs). After skin preparation, epidermal cell suspensions were isolated and incubated with Alexa-546-labeled nanoparticles (A546-nanoparticles). (**a**) Representative FACS gating strategy. Arrows indicate the sequence of steps. First, cells are discriminated from debris on the basis of forward (FSC-A) and side scatter (SSC-A) characteristics (top left panel). Second, dead cells are excluded from further analysis by their 7AAD positivity (lower left panel). Third, within viable CD45-negative cells (that is, keratinocytes; upper middle panel) and viable CD45+ cells (lower middle panel) doublets are identified by their FSC-W and FSC-H properties and are omitted from further analysis. Doublets are the cells outside the gated area; about 20%. Single cells (about 80%) are within the gate. Fourth, epidermal cells are defined as MHC-II$^-$/CD3$^-$ keratinocytes (upper right panel) and MHC-II$^+$/CD3$^-$ LCs and MHC-II$^-$/CD3$^+$ dendritic epidermal T cells/DETC (lower right panel). (**b**) Representative FACS contour plots (upper row) and histogram overlays (lower row) of keratinocytes, dendritic epidermal T cells and CD40$^+$ LCs show the uptake of nanoparticles. Histogram overlays (lower row) show the uptake of Alex-546-conjugated nanoparticles (dark gray lines) compared with control cultures without nanoparticles (light gray lines). Representative FACS plots are shown of four individually analyzed mice per group.

© 2014 Macmillan Publishers Limited

LCs preferentially capture the vaccine

Ex vivo cultures of murine epidermal cells were employed to investigate the uptake of the nanoparticles by LCs. Alexa-546-labeled nanoparticles added to the cell culture were captured by more than 90% of the MHC class II-positive LCs. These LCs become activated by the nanoparticles because they expressed the costimulatory molecule CD40 (Figure 1b). In contrast, keratinocytes were inefficiently loaded with nanoparticles and epidermal T cells were devoid of nanoparticles (Figure 1). The nanoparticles had undetectable cytotoxicity. These results indicate that LCs preferentially capture the nanoparticles.

Transgene expression in LCs was investigated by nanoparticles made with a pDNA encoding the green fluorescent protein (GFP). These nanoparticles were applied onto the prepared skin of BALB/c mice, and then isolated epidermal cells were analyzed by flow cytometry (Table 1). In the negative control samples, 0.3% of the cells were green. In the positive control samples, subcutaneous injection of fluorescein isothiocyanate-dextran resulted in 15.9% green cells.[14] For mice treated with the pDNA/PEIm nanoparticles on the surface of the skin, 9.4% of the cells expressed GFP. After subcutaneous injection of the nanoparticles only 0.8% of the cells expressed GFP. These data suggest that the pDNA/PEIm nanoparticles effectively transduce LCs after topical administration and poorly after injection.[15]

Loading the vaccine into the epidermis

For LC-targeting vaccination, we needed to deliver the nanoparticles to the proximity of LCs in the epidermis. We applied Alexa-514-labeled nanoparticles on either exfoliated or intact dorsal BALB/c mouse skin, and 3 h later, we examined the different layers of the skin with scanning two-photon (2P) absorption fluorescence microscopy (Figure 2). In the intact (shaved) skin, most of the nanoparticles remained on the surface, albeit a small fraction penetrated into the upper layers of the epidermis. We found that exfoliation facilitated the penetration of nanoparticles into the epidermis. These nanoparticles formed a deposit at a depth of 50–110 μm. These experiments showed that skin exfoliation and barrier disruption is essential for efficient loading of the nanoparticles into the epidermis, in the close proximity of LCs.

Table 1. Gene expression in LCs loaded *in vivo* with pDNA/PEIm nanoparticles

Material	*Administration*	*% of fluorescent cells*
Glucose	Transdermal	0.3
Nanoparticles	Transdermal	9.5
Nanoparticles	Injection	0.8
FITC-dextran	Injection	15.9

Abbreviations: FITC, fluorescein isothiocyanate; LC, Langerhans cell.

Visualization of the LC-targeting vaccination in live animals

We have assembled a non-invasive device suitable to examine the fate of the nanoparticles inside the skin *in vivo*. This is a near infrared 2P absorption fluorescence laser scanning microscope (TPLSM) used in combination with advanced image analysis software. For visualization of the LCs in the skin of a living animal, we used a knock-in mouse model expressing enhanced GFP (eGFP) under the control of the Langerin (*CD207*) gene.[16] We established that the 2P emission of Alexa-546-labeled nanoparticles excited at wavelength of $\lambda_0 = 890$ nm is optimal at 550–600 nm ('red' non-descanned channel) and marginal at 500–550 nm ('green' non-descanned channel). During our initial experiments we found that the eGFP signals of LCs are not detectable in the 'red' non-descanned channel, suggesting that the green emission of LCs does not disturb the detection of the red emission of the nanoparticles (Figure 3a).

We compared the images of LC-containing layers of intact and exfoliated epidermis with images of epidermis 3 and 24 h after administration of nanoparticles. We observed that LCs in intact skin displayed thin and branched dendrites as described earlier (Figure 3a).[16] Notably, most LCs in intact skin specifically captured nanoparticles that penetrated through the epidermis (Figure 3b). This result confirmed our previous observations indicating that a small amount of nanoparticle could penetrate intact skin (Figure 2). The morphology of nanoparticle-loaded LC in the intact skin did not remarkably changed over a period of 24 h. LC activation and nanoparticle uptake were different in the exfoliated skin. All LCs in the exfoliated skin picked up nanoparticles. Three hours after skin treatment, LCs presented the classical dendritic morphology that changed to a more rounded, less branched phenotype after 24 h, in accordance with previous data on tape stripping (Figure 3c).[16] Interestingly, 3 h after nanoparticle administration onto the exfoliated skin, all LCs underwent significant morphologic changes showing rounded cell bodies with fewer, thicker, shorter and non-branched dendrites, a sign of motility and activation (Figure 3d). This occurred at least 21 h faster compared with skin exfoliation alone, without nanoparticle administration. Moreover, skin exfoliation increased the uptake of nanoparticles. The amount of nanoparticles in the LCs was greater in the exfoliated skin compared with the intact skin (Figure 3e vs Figure 3f). We did not observe nanoparticles in any of the surrounding cells (for example, keratinocytes). These results demonstrate the specificity of the LC-targeting vaccination. In addition, these high-resolution images demonstrated the first time perinuclear/nuclear localization of the nanoparticles in LCs suggesting that targeted delivery of pDNA into the nucleus of LCs was achieved *in vivo* (Figures 3e and f). Our data suggest that the combination of skin exfoliation and nanoparticle administration is required for both optimal LC-targeting DNA delivery and optimal activation of LCs to migrate to the lymph nodes.

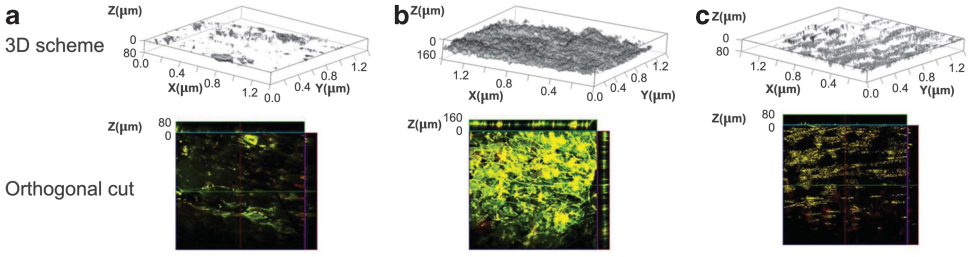

Figure 2. Penetration of pDNA/PEIm nanoparticles into the skin. (**a**) Dorsal skin of control BALB/c mice without skin exfoliation and nanoparticle application. (**b**) Application of Alexa-514-labeled nanoparticle onto the surface of exfoliated dorsal skin of mice. Penetration depth is 50–110 μm. (**c**) Application of Alexa-514-labeled nanoparticles onto the surface of shaved skin. Penetration depth is 1–40 μm.

© 2014 Macmillan Publishers Limited

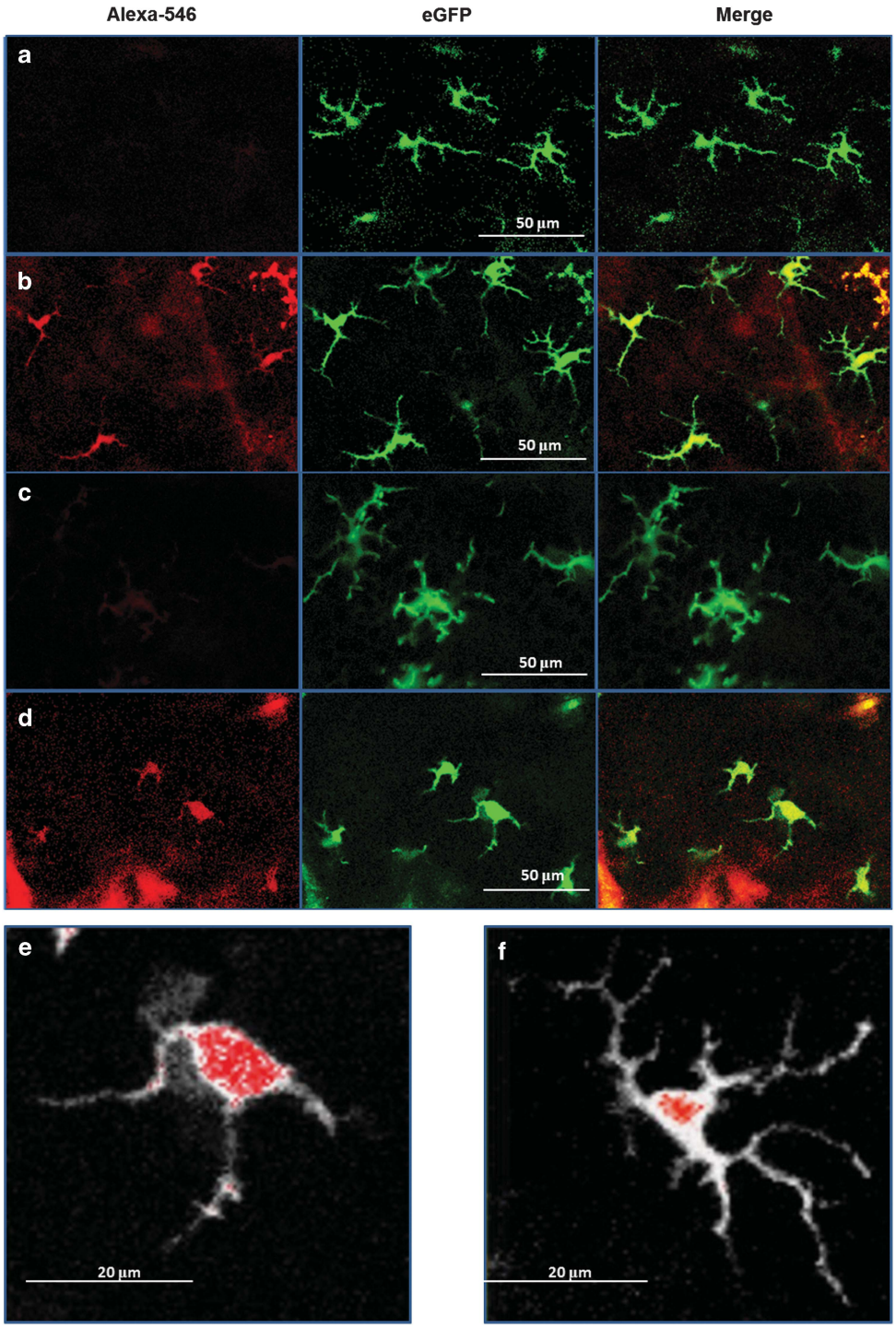

Figure 3. Real-time visualization of the incorporation of Alexa-546-labeled nanoparticles by LCs in living eGFP-Langerin knock-in mouse after 3 h. (**a**) Control (intact) skin; (**b**) nanoparticles applied onto intact skin; (**c**) exfoliated skin; (**d**) nanoparticles applied onto exfoliated skin; (**e**, **f**) images showing the morphology of representative LCs (white) with nanoparticles (red); (**e**) a motile LC with nanoparticles after skin exfoliation; (**f**) resident LC with nanoparticles in intact skin. The green channel was gray scaled and the red channel was merged with the gray image.

Topical vaccination increases the migration of LCs

Z-stack analysis of the epidermis with TPLSM is suitable for the *in vivo* detection of the initiation of LCs migration to the lymph nodes. For these migration studies, three-dimensional (3D) image stacks were acquired every 6 min for 48 min using 14 sections in a 28-µm penetration depth. We investigated the vertical movement of LCs by analyzing the appearance or disappearance of LCs in the same skin layer at different time points (Figures 4a and b). Our results confirmed previous observation indicating that most of the LCs were resident in the intact and in the exfoliated skin. In contrast, exfoliation and nanoparticle administration together increased the motility of LCs by fivefold. LC migration was documented by the appearance or disappearance of about 48% (SD = 22%) of LCs in 38 min, in the observed zone. Interestingly, nanoparticle

© 2014 Macmillan Publishers Limited

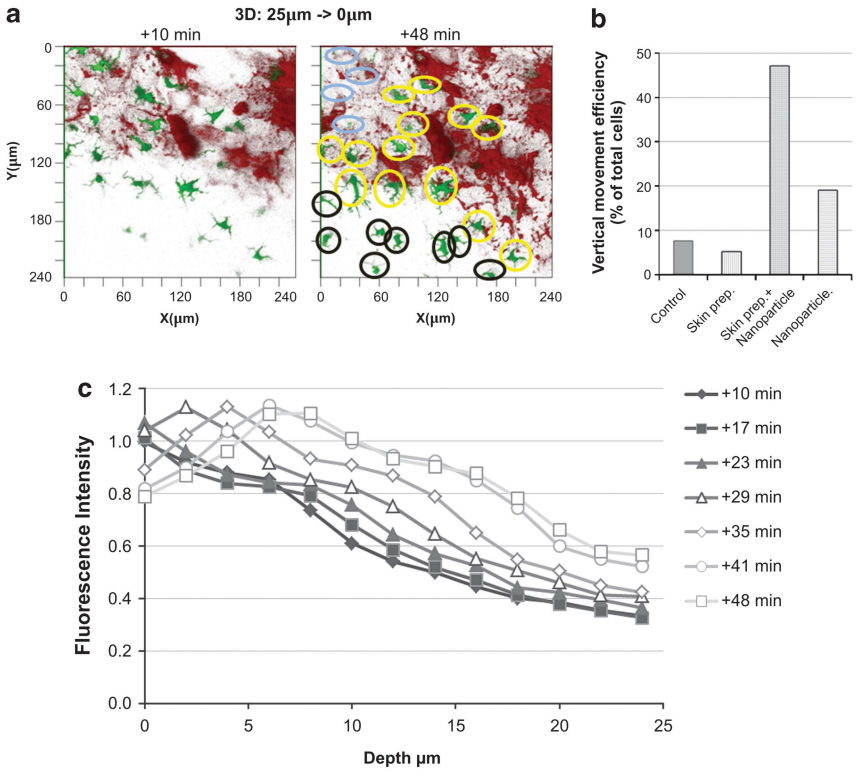

Figure 4. Motility of LCs in the epidermis of eGFP-Langerin knock-in mouse after 2 h. (**a**) The representative Z-stack layer of a mouse skin +10 and +48 min after skin exfoliation and nanoparticle administration demonstrating an example for the vertical movement of LCs. Analysis were performed by counting the appearing (black circles), disappearing (blue circles) and remaining cells (yellow circles) after +48 min compared with the cells present in the same skin +10 min. Field: $240 \times 240\ \mu m^2$. (**b**) Vertical movement efficiency of LCs after different treatments. (**c**) Migration kinetics of nanoparticle-loaded LCs after combined administration of skin treatment and nanoparticles. Merged intensities (yellow) of eGFP (green) and Alexa-546 (red) were calculated in every Z-axis profile at every time point, representing each line.

administration on intact skin also resulted in a twofold increase of LC motility, suggesting that the process of nanoparticle capture alone may provoke the migration of LCs (Figure 4b).

To characterize the migration kinetics of vaccine-loaded LCs, we developed a software that calculates the merged intensities (yellow) of eGFP and Alexa-546 fluorescence at every skin layer and every time points. Figure 4c demonstrates the vaccine-loaded LCs within skin layers in consecutive time points, where the fluorescent intensity is proportional with the number of vaccine-loaded LCs, the depth is the distance of the analyzed skin layer from the surface, and the time points represent the time after vaccine application. The analysis revealed that vaccine-loaded LCs migrated into the deeper layers of the skin as demonstrated a shift of the maximum intensities in time from the upper layers of the skin toward the deeper layers. The ~20% decrease of fluorescent intensity in the upper layers of the skin indicate that vaccine-loaded LCs were rapidly exiting from the skin. Quantitative analysis showed that ~30% of vaccine-loaded LC left the skin in 48 min after vaccination (Supplementary Figure 2).

These results demonstrate that the combination of exfoliation and nanoparticle administration is required for the potent initiation of migration of the vaccine-loaded LCs to the lymph nodes.

Localization of the DNA in draining lymph nodes

We investigated the tissue distribution of the pDNA after LC-targeting vaccination in New Zealand White Rabbits 7, 30 and 60 days after treatment (Figure 5). Seven days after a single topical application of the nanoparticles to the exfoliated skin, 56% of the penetrated nanoparticles (average 421 pDNA copies/100 ng chromosomal DNA; SD% = 127) were detected in the skin-draining lymph nodes (axillary, popliteal, inguinal, iliac, mesenteric lymph nodes), suggesting that nanoparticle-loaded LCs migrated to the lymph nodes (Figure 5a). These results confirm and quantify our previous findings on expression of antigens encoded on pDNA in the lymph nodes of mice and macaques.[17] We found 32% of the nanoparticles (average 158 copies/100 ng DNA; SD% = 222) in the treatment-site muscle. This amount might reflect a contamination of the muscle with nanoparticles during the removal of the skin. Nanoparticles were undetectable in bone marrow suggesting that cells in the dermis, especially neutrophils, are not involved in the uptake of nanoparticles.[18] Nanoparticle distribution in plasma, whole blood, kidney, heart, brain, thymus, spleen, lung, liver and genitalia ranged from 0.3 to 6%. A separate rabbit cohort was killed 30 days after LC-targeted vaccination. In these rabbits, the same tissue distribution pattern was observed despite decreased tissue pDNA levels. Forty-seven percent of the penetrated nanoparticles were detected in the lymph nodes (average 36 pDNA copies/100 ng DNA; SD% = 105). The quantity of detectable nanoparticles further decreased after 60 days, with only sporadic weak positive signals detectable in the lymph nodes (average 17 pDNA copies/ 100 ng DNA; SD% = 200). No pDNA was detected in the control animals at any time. The calculated *in vivo* half-life of the nanoparticles in the lymph nodes was 11.4 days, indicating that the pDNA does not persist in the lymphoid tissues (Figure 5b).

Clinical translation of LC-targeting vaccination

For the animal experiments, we used sedated animals for skin treatment and to administer the liquid nanoparticles on the skin surface. For human use, we needed a mechanism that maintained the contact between the prepared epidermal surface and the vaccine. We developed a new medical device, called DermaPrep, indicated for topical administration of liquid formulations

© 2014 Macmillan Publishers Limited

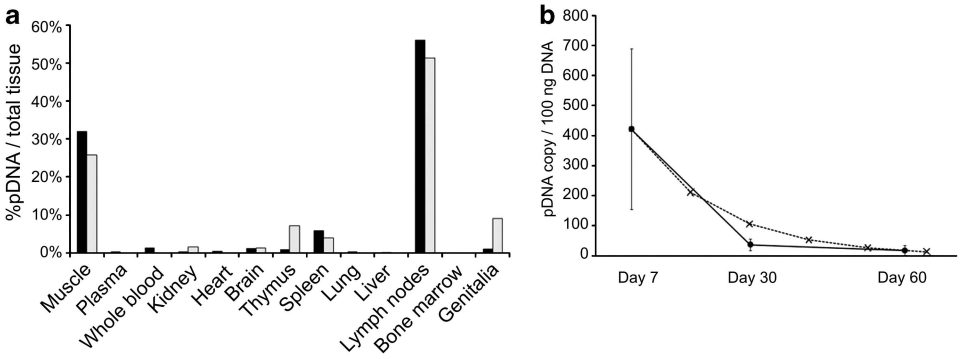

Figure 5. Tissue distribution of pDNA in New Zealand White Rabbits after topical pDNA/PEIm nanoparticle vaccination with DermaPrep. (**a**) Percentage of pDNA in 10 rabbits per test days (black bars: test day 7; gray bars: test day 30). (**b**) Average copy numbers of pDNA detected in the lymph nodes on days 7, 30 and 60 (circles and solid line). Calculated elimination rate of the nanoparticles from the lymph nodes (x and dashed line).

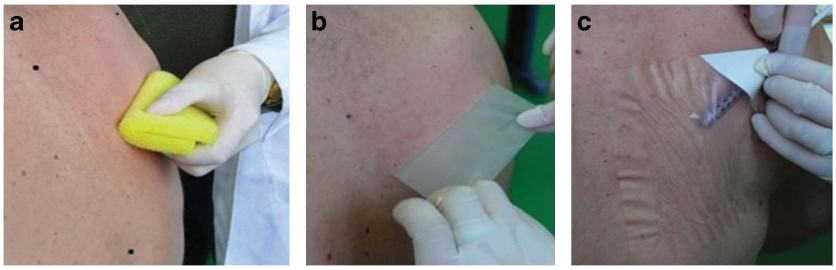

Figure 6. DermaPrep administration of liquid vaccine. (**a**) The skin treatment starts with shaving and disinfection, then the body sponge is used to exfoliate the epidermis. (**b**) Tape stripping for the removal of the residual skin material (for example, dead cells). (**c**) Transparent film (the 'patch') designed to keep liquid vaccine in contact with the exfoliated epidermis for several hours without leaking. Liquid vaccine administered under the patch is completely dried after 3 h, potentially improving the degree of penetration seen in earlier animal experiments where the liquid nanoparticles were dried within 30 min without the use of the patch.

including the LC-targeting vaccine described here. It consists of three components assembled in a pouch: a body sponge (same material as used for mice and rabbits), medical tape and an 80 cm^2 transparent film dressing (patch). Each component has well-defined functions to facilitate a mild epidermal injury in the absence of scar formation, critical for efficient loading of the vaccine into the epidermis. Liquid vaccine administered under the patch are completely dried after 3 h, potentially improving the degree of penetration seen in the animal experiments where the liquid nanoparticles were dried within 30 min without the use of the patch. Administration of the liquid vaccine with DermaPrep consists of four steps: reproducible and standardized epidermis preparation, patch application, loading of the liquid vaccine under the patch and patch removal (Figure 6).

Regulatory agencies require preclinical safety testing of the LC-targeting vaccination before clinical trials. We performed two placebo-controlled studies on New Zealand White Rabbits that included four and eight consecutive vaccine administrations with DermaPrep (Supplementary Figure 3). The primary observation after four treatments was local skin irritation with slight erythema (Draize score grade 1 in $<50\%$ of total skin sites) and well-defined erythema (Draize score grade 2 in $<5\%$ of total skin sites; Supplementary Figures 3a and b).[19] There were no differences between erythema severity observed immediately following the skin treatment and 3 h after patch removal, suggesting that skin treatment caused the desired slight epidermal injury. No edema was observed (Draize score grade 0; in 98–100% of total skin sites). Similar results for erythema and edema severity and occurrence rates were observed after eight vaccine doses (Supplementary Figures 3c and d). Erythema was transient with recovery occurred within 24–72 h. Interestingly, the skin recovery periods were shorter for subsequent LC-targeting vaccinations. The epidermis required 72 h to fully recover following the first topical vaccination. After the second and third vaccinations, all skin sites recovered to normal within 48 and 24 h, respectively. The recovery period remained 24 h following the fourth and subsequent vaccinations (Supplementary Figure 3e).

All the animals exhibited slight body temperature increases following patch removal. There were no changes in body weight, food consumption, ophthalmologic effects, autoantibody responses, urinalysis, gross necropsy examinations or organ weights. There were no apparent systemic blood chemistry or hematology toxicities.

DISCUSSION

We demonstrated the mechanism of action of the clinically proven LC-targeting DNA vaccination technology in *ex vivo* epidermal cell cultures and *in vivo* in live animals. We showed that both skin exfoliation and nanoparticle administration were required for optimal loading of the vaccine into the LC and for potent activation of the vaccine-loaded LC to migrate into the lymph nodes. Biodistribution studies demonstrated half of the penetrated vaccine in the draining lymph nodes. Preclinical safety studies on repeated vaccinations on the same skin sites showed transient erythema as the major side effect.

We demonstrated that 50–240 nm size range of the pDNA/PEIm nanoparticles, corresponding to the size range of viruses, supports receptor mediated entry to LCs.[13,20] The mannose residues on the surface of these nanoparticles also resemble the surface of viruses that carry similar glycoprotein residues recognized by LCs.[21] This vaccine effectively penetrated into the epidermis after a mild skin exfoliation and formed a deposit. Unexpectedly, preferential and efficient uptake of the nanoparticles by LCs occurred not only in the exfoliated but also in the intact mouse skin. These findings

© 2014 Macmillan Publishers Limited

might be explained by the bimodal size distribution of the nanoparticles with different penetration capability, and/or by the function of the LCs to sample the environment to pick up pathogens including mannosylated nanoparticles.[22,23] However, because human stratum corneum has a greater thickness compared with the mouse one, it is unlikely that these nanoparticles could also penetrate into the intact human skin.[24]

Nanoparticle uptake by LCs is only part of the complex mechanism of vaccine delivery to the lymph nodes via LCs. We found that nanoparticles penetrated into the intact skin. LCs in the intact skin picked up the nanoparticles but they did not considerably change their morphology or motility. These results indicate that nanoparticle alone poorly stimulate LCs to mature and vaccine-loaded LC migration to the lymph nodes in the absence of exfoliation might be slow and inefficient. These results are in agreement with previous findings showing that pDNA/polyethyleneimine complexes remained at the vaccination site after delivery with either needle injection or Biojector, but these complexes are detectable in the lymph nodes after intravenous injection.[25,26] We demonstrated that skin preparation alone was not sufficient to induce rapid morphological changes of LCs, the first sign of motility. This is in good agreement with previous findings with tape stripping where LCs became motile after 16 h, indicating that skin exfoliation is required to induce a mild skin injury (inflammation) and activate LCs to migrate to the lymph nodes.[16]

Achieving migration of DCs into the lymph node represents one of the main challenges for cancer vaccines because antigen expression in the lymph nodes is necessary to induce effective $CD8^+$ and $CD4^+$ T-cell responses. Here we demonstrated potent transgene expression in epidermal LCs after topical application of the nanoparticles. These data confirmed previous studies showing transgene expression in lymph nodes with reverse transcription-PCR, *in situ* hybridization and immunohistochemistry in mice and macaque models.[17] LC-targeting DNA vaccines express the DNA-encoded antigens in the lymph nodes and present several hundreds of epitopes on the patients' HLA molecules for direct-priming of naive T cells. In contrast, the very poor antigen expression in LCs obtained after injection suggests a different mechanism of action. Injected DNA vaccines are optimized for *in situ* protein expression at the injection site.[17] DCs pick up the expressed proteins, similar to injected protein vaccines, and cross-prime naive T cells, consequently DNA could only be sporadically found in the lymph nodes.[26,27] Therefore, the direct-priming of CTL responses employed by LC-targeting DNA vaccination seems to be superior to vaccination technologies that exploit cross-priming (gene gun, DNA injection, protein with adjuvants, and so on).

We clarified the mechanism of action in both *ex vivo* and *in vivo* settings demonstrating that nanoparticles-loaded LCs get activated in the skin to migrate into the lymph nodes. Previous studies showed that PEI-based nanoparticles upregulate the costimulatory markers of CD40 and CD86 *in vitro* and *in vivo*.[28,29] We found that all the LCs in epidermal cell culture captured the nanoparticles and expressed costimulatory molecules demonstrating the state of activation. This finding is supported with *in vivo* results showing phenotypic activation of nanoparticle-loaded LCs (Figure 3d). In live animal setting, we showed that optimal LC activation and migration required both pDNA/PEIm formulation and topical administration of the nanoparticles after exfoliation of the skin.

Tremendous efforts have been put into the design of maturation cocktails mimicking pathogen-derived molecular activations.[30] The LC-targeting vaccination technology provides an *in vivo* solution to this challenge. We found that half of the penetrated vaccine was localized in the skin-draining lymph nodes. Here we demonstrated that *in vivo* stimulation of LCs, with appropriate vaccine formulation and skin treatment, was required for the rapid initiation of migration of vaccine-loaded LCs to the lymph node. This observation further supports the potency of the vaccination technology mimicking the natural pathway for LC activation and consequent lymph node delivery of pathogen-derived antigens. Therefore, LC-targeting vaccination might improve the potent but cumbersome *ex vivo* DC-based vaccination methods used for infectious diseases and cancer treatment.[31–33]

Many DNA vaccines proved to be immunogenic and effective in animal models, but translation of these results to human vaccines has been unsuccessful. One common translational problem is that the vaccine dose administered to mice cannot be scaled up to humans. LC-targeting vaccination technology might solve this translation challenge by administering the vaccine topically onto the prepared skin. The skin has only a slightly variable LC density in different mammals (a 900–1 800 cells per mm^2 horizontal network under the skin surface).[34] Therefore, the dose escalation can be achieved by targeting DNA to different lymph nodes simultaneously after applying the vaccine on differently sized and located skin surfaces.[11]

There are concerns about the toxicity of pDNA/PEI nanoparticles.[35] Mortality was described in different strains of mice after intravenous administration of 50 μg pDNA nanoparticles.[36] Importantly, the LC-targeting pDNA/PEIm vaccine as safe as placebo and induced potent and long-lasting memory CTL responses in human subjects.[11] Therefore, toxicity obtained with different formulations and administration routes cannot be extrapolated. One reason for the conflicting toxicities observed might be due to the different PEIs used in nanoparticle formulations. These polymers can have either a branched- or linear-structure and a wide-range of molecular weights from 0.4 to 800 kDa. Another potential reason may be that the physiological salt concentration of the blood causes aggregation of the nanoparticles and drastically increases their size.[12] Such aggregation occurs after intravenous injection.[37] However, even under these circumstances, the 22-kDa molecular weight PEI used for the formulation of pDNA/PEIm nanoparticles had lower toxicity than 800 kDa PEI.[38,39] Our studies demonstrated that DermaPrep skin preparation supported the safe and effective loading of the pDNA/PEIm nanoparticles into LCs. Two preclinical safety studies conclusively showed that toxicity of the LC-targeting vaccination was limited to a clinically acceptable mild erythema. These features make the LC-targeting vaccination technology a relevant CTL-inducing cancer vaccine product candidate in human subjects.

Vaccine development has entered into the era of rational design. The distinct functional capacities of different DC subsets are being harnessed.[40] By preferentially and effectively targeting antigens to LCs, a cell type critically implicated in CTL induction and anti-cancer immune responses, the described technology and approach holds promise for the future.

MATERIALS AND METHODS

Experimental design

Skin penetration studies in living animals. Nanoparticle penetration studies were performed on anesthetized Lang-EGFP mice (a knock-in mouse model expressing eGFP under the control of the Langerin (*CD207*) gene[16]). Skin samples were excised and were investigated by TPLSM for the presence of labeled nanoparticles in the epidermal cell layers as well as for the morphologic and motility changes of LCs induced by the nanoparticles ($n = 3$).

Tissue distribution after topical delivery of nanoparticles. A single topical vaccine treatment was performed on 42 white New Zealand White Rabbits in a GLP study. Thirty animals received nanoparticle solution containing pDNA-encoding HIV genes (DermaVir) and twelve animals received control solution.[40] Animals were killed on days 7, 30 or 60 for quantitative PCR detection of pDNA distributed in organs and tissues. Four parallel quantitative PCR reactions were made for each tissue sample.

© 2014 Macmillan Publishers Limited

Safety studies with topical vaccine treatment. Topical vaccine treatment was performed according to the human protocol (http://www.geneticimmunity.com/) in a GLP study. Twenty New Zealand rabbits were treated with 0.8 ml nanoparticles in glucose solution under two patches. The control group received only glucose. Three hours (that is, immediately after removal of the patch), 24, 48, and 72 h after treatments the skin sites were graded by a blinded operator according to the Numerical Grading System for Treatment Site Irritation.[19]

Preparation and characterization of the nanoparticles

PEIm (polyethyleneimine mannose containing 3% mannose residues calculated to amino groups) was labeled with Alexa-546 or -514 (Invitrogen, CA, USA). Nanoparticles were prepared with pDNA-encoding HIV-1 genes of DermaVir[17] or pDNA encoding the Green Fluorescence Protein and PEIm as described previously.[41] Size distribution were performed with Brookhaven ZetaPALS at 25 °C. For atomic force microscopy (Bioscope I with Nanoscope IV controller, Veeco, Somerset, NJ, USA), the nanoparticle solution was dried on APS-mica. Imaging was made in air in tapping mode.[13] Based on previous AFM measurements the PEI coats one molecule of pDNA, which means that 0.1 mg pDNA (12.5 kBp » 8 MDa) corresponds to 7.5×10^{12} nanoparticles, that is, the concentration of nanoparticles is 9.3×10^{12} nanoparticle per ml formulation.[13]

Animals

General procedures for animal care and housing were in accordance with the National Research Council (NRC) *Guide for the Care and Use of Laboratory Animals* (1996) and the Animal Welfare Standards. Rabbits and mice were anesthetized using sodium pentobarbital administered intravenously or intraperitonally. TPLSM studies were approved by the Semmelweis University Animal Care and Use Committee.

Topical vaccination of mice

Topical vaccine treatment was performed according to the human protocol (http://www.geneticimmunity.com/IFU) using the same materials except transparent film (the patch): (a) the skin treatment starts with shaving and disinfection, then the body sponge is used to exfoliate the epidermis; (b) tape stripping for the removal of the residual skin material (for example, dead cells); liquid vaccine administered on the skin and left to completely dry for 30 min.

Epidermal cell culture, gene expression and flow cytometry

Seven million murine epidermal cells were isolated and cultured with Alexa-546-labeled nanoparticles as described previously.[42] After 20 h, samples were stained using antibodies against MHC class II (clone M5/114.15.2, eBioscience, Vienna, Austria), CD40 (clone 3/23, Becton Dickinson, San Jose, CA, USA) and CD45 (clone 30-F11, eBioscience) and analyzed on a FACSCantoII flow cytometer (Becton Dickinson). Dead cells were excluded by co-staining with 7AAD (Becton Dickinson). About 1% of the MHC class II-positive cells were dead in the nanoparticle-treated samples, and about 0.7% in the untreated controls. A minimum of 200 000 events was acquired for each measurement. FACS data were analyzed with FlowJo software (Three Star, Ashland, OR, USA).

For gene expression experiments 6 h after skin preparation and nanoparticle administration, the mice were killed, the skin was removed and cultured as described previously. The cells that migrated out from the skin into the culture media were harvested and the large cells containing the LC population were analyzed using flow cytometry.

Skin penetration studies with Z-stack analysis

For nanoparticle penetration studies, anesthetized BALB/c mice were killed after 3 h of Alexa-514-labeled nanoparticle treatment. Skin samples were excised and for 2P excitation of the Alexa-514 dye, a mode-locked Yb-fiber laser ($\lambda_0 = 1030$ nm, $\tau = 300$ fs) was used. 3D image stacks were acquired ($1500 \times 1500 \times 80\ \mu m^3$) using 10 sections and magnification of ×40. Excitation was 1030 nm.

Studies on living mice with femtosecond TPLSM

Anesthetized *Lang-EGFP* mice were laid on the heated microscope-table and the ears of mouse were fixed to microscope slide and examined with TPLSM that we have assembled. For 3D measurements, a femtosecond pulse Ti-sapphire laser generates nearly transform limited, $\tau_{FWHM} \sim 190$ fs pulses at a repetition rate of ~ 76 MHz.[43] The laser utilizes ultra broadband chirped mirror technology for broad tunability (690–1050 nm) without changing the cavity optics.[43] The laser central wavelength was set to ~ 910 nm, which assures high 2P excitation efficiency for both the Alexa-546-labeled nanoparticles and the eGFP-labeled LCs, but low background autofluorescence signal from the intrinsic autofluorescent molecules in the skin.[44] For 3D imaging, we used a two-channel, Axio Examiner LSM 7MP microscope (Carl Zeiss, Jena, Germany). Scanning in the *x–y* plane was achieved with galvanometer mirrors. Subfemtolitre excitation beam focusing was achieved using a high-numerical aperture (NA ~ 1.0) x40 water immersion objective (Zeiss), with a working distance of about 1 mm. Stepper motor control of the objective lens focus enabled scanning along the optical *z*-axis with a minimum step size of 150 nm. The average power of the laser beam reaching the sample is typically set to ~ 10 mW by a built-in acousto-optic device, which assures thermal damage-free excitation. For cross-talk-free recording of the flourescence signals, two bandpass filters and a corresponding dichroic filter were placed in front of the non-descanned detectors: BPF1 (green) and BPF2 (red) filters having transmission bands in the 500–550 nm and the 565–610 nm wavelength regimes.

For LC migration studies, 3D image stacks were acquired every 6 min for 48 min using 14 sections, 28 μm skin penetration and a magnification of x40. For the estimation of vertical movement of LCs, a percentage rate was established: count (sum) of the newly appearing and disappearing cells divided by the total number of cells observed in the field. LSM software was used for image processing.

Tissue distribution after topical delivery of nanoparticles

A single topical vaccine treatment was performed on 42 white New Zealand rabbits. Thirty animals received 0.8 ml nanoparticle solution containing pDNA-encoding HIV genes (DermaVir) and twelve animals received 0.8 ml of control solution.[40] Animals were killed on days 7, 30 or 60 for quantitative PCR detection of pDNA distributed in organs and tissues. Half-life is calculated following the equation: Half-life = (elapsed time*log2)/log(beginning amount/ending amount).

From 23 tissue samples per rabbit, genomic DNA were purified (DNeasy, Qiagen, Valencia, CA, USA). Four parallel quantitative PCR reactions were made for each tissue sample. The blank control was water. Detection limit was established as 10 copies per 100 ng genomic DNA. Primer1: 5′-ATAA TCCACCTATCCCAGTAGGAGAAAT-3′; Primer2: 5′-GGTCCTTGTCTTATGTC CAGAAxTGC-3′, where x is a Lightcycler Red640 flurophore; probe 5′-TAAATAAAATAGTAAGAATGTATAGCCCTACCAGC-fl-3′. Conditions are as follows: denaturing step for 10 min at 95 °C, followed by 55 cycles of amplification (95 °C for 10 s, 55 °C for 10 s, 72 °C for 5 s), and ending with a melting cycle of continuous increase in temperature up to the target temperature of 80 °C.

CONFLICT OF INTEREST

JL, ERT, ZC, OL, ES, LM, FL hold shares in Genetic Immunity Inc. The remaining authors declare no conflict of interest.

ACKNOWLEDGEMENTS

We thank Drs Michael A Ussery and Hao Zhang (Division of AIDS, NIAID) for their support. The study was supported by NIH (N01-AI-70043) and Hungarian National Office for Research and Technology (FIBERSC2, contract no. TECH-09-A2-2009-0134 and DVCLIN01). FH acknowledges the support of the Intramural Research Program of the NICHD, NIH. CHT was in part supported by the COMET Center ONCOTYROL (Cell Therapy Unit), which is funded by the Austrian Federal Ministries for Transport, Innovation and Technology, and Economics, Family and Youth (via the Austrian Research Promotion Agency / FFG) and the Standortagentur Tirol.

REFERENCES

1 Steinman RM. Decisions about dendritic cells: past, present, and future. *Annu Rev Immunol* 2012; **30**: 1–22.
2 Stoitzner P, Green LK, Jung JY, Price KM, Tripp CH, Malissen B *et al.* Tumor immunotherapy by epicutaneous immunization requires langerhans cells. *J Immunol* 2008; **180**: 1991–1998.
3 Banchereau J, Thompson-Snipes L, Zurawski S, Blanck J-P, Cao Y, Clayton S *et al.* The differential production of cytokines by human Langerhans cells

© 2014 Macmillan Publishers Limited

and dermal CD14(+) DCs controls CTL priming. *Blood* 2012; **119**: 5742–5749.
4 Romano E, Cotari JW, Barreira da Silva R, Betts BC, Chung DJ, Avogadri F *et al.* Human Langerhans cells use an IL-15R-α/IL-15/pSTAT5-dependent mechanism to break T-cell tolerance against the self-differentiation tumor antigen WT1. *Blood* 2012; **119**: 5182–5190.
5 Romani N, Thurnher M, Idoyaga J, Steinman RM, Flacher V. Targeting of antigens to skin dendritic cells: possibilities to enhance vaccine efficacy. *Immunol Cell Biol* 2010; **88**: 424–430.
6 Zaric M, Lyubomska O, Touzelet O, Poux C, Al-Zahrani S, Fay F *et al.* Skin dendritic cell targeting via microneedle arrays laden with antigen-encapsulated poly-d,l-lactide-co-glycolide nanoparticles induces efficient antitumor and antiviral immune responses. *ACS Nano* 2013; **7**: 2042–2055.
7 Stoitzner P, Sparber F, Tripp CH. Langerhans cells as targets for immunotherapy against skin cancer. *Immunol Cell Biol* 2010; **88**: 431–437.
8 Combadière B, Vogt A, Mahé B, Costagliola D, Hadam S, Bonduelle O *et al.* Preferential amplification of CD8 effector-T cells after transcutaneous application of an inactivated influenza vaccine: a randomized phase I trial. *PLoS One* 2010; **5**: e10818.
9 Diebold SS, Kursa M, Wagner E, Cotten M, Zenke M. Mannose polyethylenimine conjugates for targeted DNA delivery into dendritic cells. *J Biol Chem* 1999; **274**: 19087–19094.
10 Lisziewicz J, Tőke ER. Nanomedicine applications towards the cure of HIV. *Nanomedicine* 2013; **9**: 28–38.
11 Lisziewicz J, Bakare N, Calarota S a, Bánhegyi D, Szlávik J, Ujhelyi E *et al.* Single DermaVir immunization: dose-dependent expansion of precursor/memory T cells against all HIV antigens in HIV-1 infected individuals. *PLoS One* 2012; **7**: e35416.
12 Rodriguez B, Asmuth DM, Matining RM, Spritzler J, Jacobson JM, Mailliard RB *et al.* Safety, tolerability, and immunogenicity of repeated doses of DermaVir, a candidate therapeutic HIV vaccine, in HIV-infected patients receiving combination antiretroviral therapy: results of the ACTG 5176 trial. *J Acquir Immune Defic Syndr* 2013; **64**: 351–359.
13 Lőrincz O, Tőke ER, Somogyi E, Horkay F, Chandran PL, Douglas JF *et al.* Structure and biological activity of pathogen-like synthetic nanomedicines. *Nanomedicine* 2012; **8**: 497–506.
14 Bruewer M, Utech M, Ivanov AI, Hopkins AM, Parkos C a, Nusrat A. Interferon-gamma induces internalization of epithelial tight junction proteins *via* a macropinocytosis-like process. *FASEB J* 2005; **19**: 923–933.
15 Sallusto F, Cella M, Danieli C, Lanzavecchia A. Dendritic cells use macropinocytosis and the mannose receptor to concentrate macromolecules in the major histocompatibility complex class II compartment: downregulation by cytokines and bacterial products. *J Exp Med* 1995; **182**: 389–400.
16 Kissenpfennig A, Henri S, Dubois B, Laplace-Builhé C, Perrin P, Romani N *et al.* Dynamics and function of Langerhans cells *in vivo*: dermal dendritic cells colonize lymph node areas distinct from slower migrating Langerhans cells. *Immunity* 2005; **22**: 643–654.
17 Lisziewicz J, Trocio J, Whitman L, Varga G, Xu J, Bakare N *et al.* DermaVir: a novel topical vaccine for HIV/AIDS. *J Invest Dermatol* 2005; **124**: 160–169.
18 Duffy D, Perrin H, Abadie V, Benhabiles N, Boissonnas A, Liard C *et al.* Neutrophils transport antigen from the dermis to the bone marrow, initiating a source of memory CD8+ T cells. *Immunity* 2012; **37**: 917–929.
19 Draize JH, Woodard G, Calvery HO. Methods for the study of irritation and toxicity of substances applied topically to the skin and mucous membranes. *J Pharmacol Exp Ther* 1944; **82**: 377–390.
20 Racoosin EL, Swanson J A. M-CSF-induced macropinocytosis increases solute endocytosis but not receptor-mediated endocytosis in mouse macrophages. *J Cell Sci* 1992; **102**: 867–880.
21 Van der Vlist M, Geijtenbeek TB. Langerin functions as an antiviral receptor on Langerhans cells. *Immunol Cell Biol* 2010; **88**: 410–415.
22 Frugé RE, Krout C, Lu R, Matsushima H, Takashima A. Real-time visualization of macromolecule uptake by epidermal Langerhans cells in living animals. *J Invest Dermatol* 2012; **132**: 609–614.
23 Kubo A, Nagao K, Yokouchi M, Sasaki H, Amagai M. External antigen uptake by Langerhans cells with reorganization of epidermal tight junction barriers. *J Exp Medi* 2009; **206**: 2937–2946.
24 So P, Kim H, Kochevar I. Two-Photon deep tissue *ex vivo* imaging of mouse dermal and subcutaneous structures. *Opt Express* 1998; **3**: 339–350.
25 Jeong G-J, Byun H-M, Kim JM, Yoon H, Choi H-G, Kim W-K *et al.* Biodistribution and tissue expression kinetics of plasmid DNA complexed with polyethylenimines of different molecular weight and structure. *J Controlled Release* 2007; **118**: 118–125.
26 Sheets RL, Stein J, Manetz TS, Duffy C, Nason M, Andrews C *et al.* Biodistribution of DNA plasmid vaccines against HIV-1, Ebola, Severe Acute Respiratory Syndrome, or West Nile virus is similar, without integration, despite differing plasmid backbones or gene inserts. *Toxicol Sci* 2006; **91**: 610–619.
27 Chen D, Payne LG. Targeting epidermal Langerhans cells by epidermal powder immunization. *Cell Res* 2002; **12**: 97–104.
28 Xun S, Ch Simu, Jianfeng H, Zhirong Zh. Mannosylated biodegradable polyethyleneimine for targeted DNA delivery to dendritic cells. *Int J Nanomed* 2012; **7**: 2929–2942.
29 Alshamsan A, Hamdy S, Haddadi A, Samuel J, El-Kadi AOS, Uludağ H *et al.* STAT3 knockdown in B16 melanoma by siRNA lipopolyplexes induces bystander immune response *in vitro* and *in vivo*. *Transl Oncol* 2011; **4**: 178–188.
30 Pilling AM, Harman RM, Jones SA, McCormack NAM, Lavender D, Haworth R. The assessment of local tolerance, acute toxicity, and DNA biodistribution following particle-mediated delivery of a DNA vaccine to minipigs. *Toxicol Pathol* **30**: 298–305.
31 García F, Climent N, Guardo AC, Gil C, León A, Autran B *et al.* A dendritic cell-based vaccine elicits T cell responses associated with control of HIV-1 replication. *Sci Transl Med* 2013; **5**: 166ra2.
32 Strioga MM, Felzmann T, Powell Jr Dr, Ostapenko V, Dobrovolskiene NT, Matuskova M *et al.* Therapeutic dendritic cell-based cancer vaccines: the state of the art. *Criti Rev Immunol* 2013; **33**: 489–547.
33 Gilboa E. DC-based cancer vaccines. *J Clin Invest* 2007; **117**: 1195–1203.
34 Bauer J, Bahmer F a, Wörl J, Neuhuber W, Schuler G, Fartasch M. A strikingly constant ratio exists between Langerhans cells and other epidermal cells in human skin. A stereologic study using the optical disector method and the confocal laser scanning microscope. *J Invest Dermatol* 2001; **116**: 313–318.
35 Goula D, Remy JS, Erbacher P, Wasowicz M, Levi G, Abdallah B *et al.* Size, diffusibility and transfection performance of linear PEI/DNA complexes in the mouse central nervous system. *Gene Therapy* 1998; **5**: 712–717.
36 Chollet P, Favrot MC, Hurbin A, Coll J-L. Side-effects of a systemic injection of linear polyethylenimine-DNA complexes. *J Gene Med* **4**: 84–91.
37 Kircheis R, Wightman L, Wagner E. Design and gene delivery activity of modified polyethylenimines. *Adv Drug Deliv Rev* 2001; **53**: 341–358.
38 Wightman L, Kircheis R, Rössler V, Carotta S, Ruzicka R, Kursa M *et al.* Different behavior of branched and linear polyethylenimine for gene delivery *in vitro* and *in vivo*. *J Gene Med* 2001; **3**: 362–372.
39 Palucka K, Banchereau J, Mellman I. Designing vaccines based on biology of human dendritic cell subsets. *Immunity* 2010; **33**: 464–478.
40 Somogyi E, Xu J, Gudics A, Tóth J, Kovács AL, Lori F *et al.* A plasmid DNA immunogen expressing fifteen protein antigens and complex virus-like particles (VLP+) mimicking naturally occurring HIV. *Vaccine* 2011; **29**: 744–753.
41 Toke ER, Lorincz O, Somogyi E, Lisziewicz J. Rational development of a stable liquid formulation for nanomedicine products. *Int J Pharm* 2010; **392**: 261–267.
42 Stoitzner P, Romani N, McLellan AD, Tripp CH, Ebner S. Isolation of skin dendritic cells from mouse and man. *Methods Mol Biol* 2010; **595**: 235–248.
43 Mayer EJ, Möbius J, Euteneuer A, Rühle WW, Szipocs R. Ultrabroadband chirped mirrors for femtosecond lasers. *Opt Lett* 1997; **22**: 528–530.
44 Breunig HG, Studier H, König K. Multiphoton excitation characteristics of cellular fluorophores of human skin *in vivo*. *Opt Express* 2010; **18**: 7857–7871.

Supplementary Information accompanies this paper on Gene Therapy website (http://www.nature.com/gt)

© 2014 Macmillan Publishers Limited